AMERICAN JOURNAL OF AGRICULTURAL SCIENCE, ENGINEERING, AND TECHNOLOGY (AJASET)

ISSN: 2158-8104 (ONLINE), 2164-0920 (PRINT)

VOLUME 7 ISSUE 2 (2023)

PUBLISHED BY: E-PALLI PUBLISHERS, DELAWARE, USA

American Journal of Agricultural Science, Engineering, and Technology (AJASET)

Volume 7 Issue 2, Year 2023
ISSN: 2158-8104 (Online), 2164-0920 (Print)
DOI: https://doi.org/10.54536/ajaset.v7i2.1063
https://journals.e-palli.com/home/index.php/ajaset

Synthesis, Corrosion Inhibition Efficiency and Adsorption Behavior of Dibenzo [a,c] Quinoxalino(2,3-I)Phenazine on Mild Steel in Acidic Medium

Olawale Matthew Akinlosotu[1*], Isaiah Ajibade Adejoro[1], Babatunde Temitope Ogunyemi[2]
Babatunde Benjamin Adeleke[1]

Article Information

Received: December 10, 2022

Accepted: April 25, 2023

Published: June 09, 2023

Keywords

Extended Pi-Conjugated Compound, Corrosion Inhibition Efficiency, Adsorption, Langmuir

ABSTRACT

Designing new inhibitors and understanding the mechanisms responsible for the inhibition are required in developing techniques to prevent corrosion. A new azaacene organic corrosion inhibitor, DQP (dibenzo[a,c]quinoxalino (2,3-i)phenazine), for mild steel in an acidic medium was successfully synthesized, characterized and reported for the first time using electrochemical impedance spectroscopy (EIS) and Potentiodynamic polarization measurement techniques (PDP). Surface morphologies and average percentage by weight of elements existing in mild steel were determined by SEM-EDX. The alterations in the impedance characteristics showed that DQP inhibitor adsorbed to the surface of mild steel, resulting in the creation of a protective coating. At the maximal concentration of 2.618 x 10^{-5} M, the inhibition efficiency reached 98.02% demonstrating DQP effectiveness in reducing corrosion process that may occur in mild steel in HCl. However, this efficiency is weakened by increase in temperature. The PDP curve revealed that DQP functions as a mixed inhibitor but is mostly cathodic. The adsorption behavior of DQP was best supported by the Langmuir adsorption isotherm (R^2 = 0.9837) while the adsorption-free energy (G^0ads) ranging from -41.749 to -43.183 kJmol^{-1} indicate chemical adsorption on metal surface. This study demonstrates that the synthesized DQP functions admirably well as a corrosion inhibitor in HCl solution.

INTRODUCTION

Iron and its alloy are the backbones of industrial constructions. Mild steel has been the most commonly employed versatile alloy in the industry for engineering applications (Prabhu *et al*., 2008) as a result of its unique and robust properties such as electrochemical and thermal conductivity high strength, lightness in weight, non-toxicity and reflectivity (Kumpawat *et al*., 2009. They are used in making medical and cutlery equipment in hospitals and food services as well as the construction of overhead tanks, pipes and valves in petroleum industry (World Steel Association, 2013). Iron and its alloys are not fundamentally stable resulting in a high tendency to revert to more stable oxidized compounds. Hence, in most environments, iron and its alloys are highly susceptible to corrosion. Corrosion is an electrochemical reaction between metal and its environment causing irreversible slow and steady degradation of both the physical and chemical properties of the metal (Sastri and Parumareddii, 1997). Commonly used methods to prevent or control metal corrosion include the adjustment of the corrosive environment, use of protective coating (metallic and non-metallic) cathodic protection, alloying of metals and the use of inhibitors. When corrosion inhibitors are added in a modest amount to the desired environment, the rate at which the environment attacks a metal is noticeably reduced (Ogunyemi and borisade, 2020; Bentis *et al*., 2002). The utilization of chemical inhibitors to slow down the corrosion process is very diverse. Organic and inorganic inhibitors have long been viewed as the first line of defense against corrosion in the oil production and refining industry. They have been the subject of several academic investigations (Li, *et al*., 2012; Obot *et al*., 2020; Adama & onyeachu 2022; Ismail *et al*., 2019). The presence of hetero atoms like Nitrogen, Oxygen, and Sulphur with multiple bonds; lone pair and pi-electrons in structures of organic compounds make good inhibitors of corrosion. However, much has not been reported about the corrosion inhibitory activities of hetero-polycyclic aromatic hydrocarbons. Most of what is known are their delightful electro-optical properties, which have many potential applications in material science (Ueda *et al*., 2014; Rao *et al*., 2016; Li *et al*., 2016; Ito *et al*., 2016; Chen *et al*., 2015). The use of PAH as an organic inhibitor of corrosion is very limited.

As an important member of the PAH family, acenes and their derivatives represent an interesting type of conjugated compounds, whose skeletons are composed of a series of linearly-fused benzene rings (Li *et al*., 2015; Sanders *et al*., 2016; Chernick *et al*., 2015; Gu *et al*., 2017). In several publications and reviews, their synthesis, characterization, and applications have been outlined (Pérez *et al*., 2013; Li *et al*., 2016; Watanabe *et al*., 2013). Therefore, in order to further enhance its use, this study focuses on the synthesis and use of DQP as an inhibitor of corrosion for mild steel in acidic media. DQP belongs to the azaacenes (N-heteroacenes) family which are derivatives of acenes in which some of the carbon atoms are replaced with more electronegative nitrogen atoms. Since the applicability and efficiency of organic

[1] Department of Chemistry, University Ibadan, Nigeria
[2] Physical and Computational Unit, Department of Chemistry, Federal University Otuoke, Bayelsa State, Nigeria
[*] Corresponding author's email: oakinlosotu50@gmail.com

inhibitors depend on their chemical structures and nature, this substitution may cause significant changes in their electronic structure that will make the synthesized compound a good and effective inhibitor of corrosion.

MATERIALS AND METHODS

Synthesis of Dibenzo [a,c] quinoxalino [2,3-i] phenazine

A mixture of 9,10-phenanthroquinone (0.2082g), 2,3-diaminophenazine (0.2214g) and Magnesium tetraoxosulphate (vi) heptahydrate (0.12940g) were dissolved in 5mL of ethanol, stirred and refluxed for two hours. Thin Layer Chromatography plate was used to monitor the reaction. After completion of the reaction, the solution was allowed to cool. The orange-brown precipitate was formed, filtered, and recrystallized from ethanol to obtain a product which was further purified using the column chromatographic method containing a solvent mixture of Ethylacetate (25%), and n-hexane (75%). The slurry of Silica gel was used as the stationary phase. The melting point of the compound was determined to be 357^{0}C-358℃

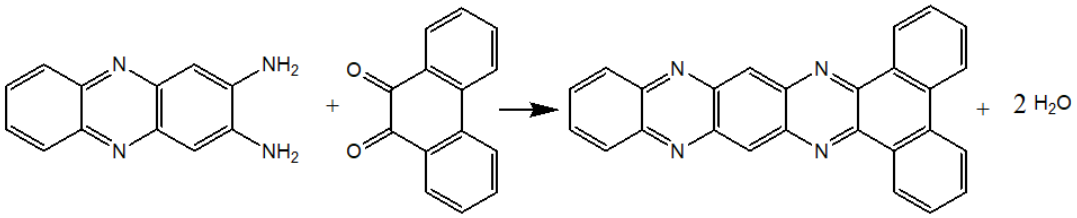

Scheme 1: Synthesis of DQP

Solution and Metal Preparation for the Experiment

Mild steel panel of 5 mm thickness and percentage composition presented in Table 1 was obtained from a Rolling mill company in Ota Ogun state and cut into coupons of dimensions 30 mm × 20 mm. The coupons' surface was polished with emery, then cleaned and degreased with acetone and ethanol. Finally, the coupons were dried in a desiccator. A 0.5 M HCl solution served as the reference corrosive substance.

Table 1: Percentage Composition of Mild Steel Panel

Element	Percentage Composition (%)
Fe	98.52
C	0.1205
Si	0.0547
Mn	0.5453
P	0.069
S	0.036
Cr	0.0804
Ni	0.2204
W	0.0329
Mo	0.0361
Cu	0.2792
Al	0.0427
Ti	0.0079
V	0.0108
Co	0.0315
Nb	0.0537
Sn	0.0028

Electrochemical Measurements

The computer-controlled AUTOLAB PGSTAT 204N.A.C electrochemical analyzer was used to carry out the electrochemical measurements. The conventional cell contained an assembly of three electrodes arrangement with a platinum sheet acting as the counter electrode. The reference electrode was Ag/AgCl (3M KCl), and the working electrode was made of mild steel. The prepared metal samples were then dipped in 0.5M HCl with and without DQP inhibitor of varying concentrations for 30 minutes.

The electrode was given permission to corrode naturally before the Potentiodynamic Polarization Measurements (Tafel) and Electrochemical Impedance Spectroscopy experiment began, and its steady-state Open Circuit Potential (OCP) with respect to time was recorded. The steady-state OCP that corresponded to the corrosion potential (E_{corr}) of the working electrode was obtained. To ascertain the current density, corrosion rate, and polarization resistance, a potentiodynamic polarization investigation was conducted from cathodic potential of -250mV to anodic potential of +250mV with a scan rate of 1.0 mVs^{-1} (Rp).

The Electrochemical Impedance Spectroscopy (EIS) was carried out with AC signals amplitude of 10 mV peak to peak in the frequency range (100 kHz-10 MHz)

Metal Surface Characterization

An Aspex 3020 Scanning Electron Microscope (SEM) and an Energy Dispersive X-ray Spectroscopy (EDS) with a 15.00 KV acceleration voltage were used to analyze the surface characteristics of the metal coupon. Mild steel coupon was dipped in 0.5 M HCl and then in test sample solutions at varied concentrations in an acidic medium. The coupons were taken out of the solutions, cleaned with acetone and deionized water, and then dried before being subjected to an SEM-EDS test. The average elemental percentage of mild steel was determined using an EDS detector connected to the SEM.

RESULT AND DISCUSSION

Potentiodynamic Polarization (PDP) Studies

The potentiodynamic polarization (PDP) test results on mild steel in 0.5 M HCl solution without and with DQP at various concentrations is shown in figure 1. Table 2 shows electrochemical variables such as current density (I_{corr}), cathode and anode Tafel gradients (βc and βa), corrosion potential (E_{corr}), corrosion rates and percentage inhibition efficiency. The findings demonstrated that when the concentration of DQP inhibitor increased, the corrosion current density (Icorr) dropped. This shows that increasing the concentration of DQP significantly reduced the rate at which mild steel corrodes (Table 2) demonstrating DQP's ability to prevent corrosion, as evidenced by the simultaneous increase in inhibition efficiency in Table 2. Higher concentrations of an inhibitor produce more soluble salts, preventing chlorides from directly attacking the steel (Patni *et al.*, 2017) by adsorbing firmly on the mild steel surface thereby covering the reaction site on the mild steel surface. The potentiodynamic polarization curve (Figure 1) clearly indicated that DQP brought about a decrease in Anodic current densities ((I_{corr}) as a result of adsorption of the DQP film on the mild steel surface. Table 2 shows the E_{corr} for the blank solution to be -537.92 mV. Upon addition of DQP inhibitor of varied concentrations, E_{corr} value ranged from -523.24 mV to -520.04 mV indicating that E_{corr} for DQP shifted towards positive potential with respect to the blank. This slight shift indicates that DQP could act as a mixed corrosion inhibitor since its corrosion potential displacement is less than 85mV when compared with the corrosion potential displacement of the blank. In addition, Table 2 reveals that the values of βc and βa were different from the values of the blank system. This indicates that DQP had changed both the anodic and cathodic processes at the same time, suggesting that DQP is a mixed-type inhibitor.

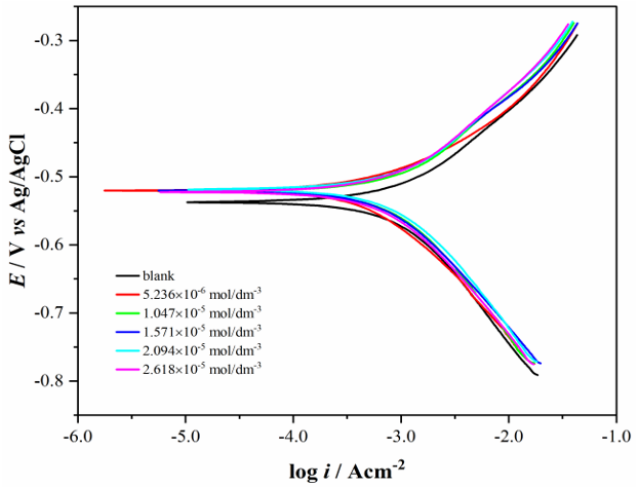

Figure 1: Potentiodynamic Polarization Curve of the Mild Steel in 0.5M HCl without and with DQP

Electrochemical Impedance Spectroscopy (EIS) Study

Another efficient method for studying the corrosion process is electrochemical impedance spectroscopy. This technique examines the impedance behavior of the study sample in 0.5 M HCl solution, both without and with DQP inhibitors. Figure 2 shows the Nyquist plot of mild steel without and with DQP. This Nyquist diagram of the study sample shows a depressed single capacitive semicircle centered under the real axis.

Table 2: Potentiodynamic Polarization Parameter for studied samples in 0.5M HCl with and without DQP

Concentration (mol/dm³)	E_{corr} (mV)	I_{corr} (μAcm^{-2})	Bc (mV)	Ba (mV)	Corrosion rate(mmpy)	(%)Inhibition efficiency
Blank	-537.92	9520.35	210.10	134.60	110.44	-
5.236 x 10^{-6}	-523.24	917.52	192.30	140.40	10.64	90.36
1.047 x 10^{-5}	-521.94	844.45	194.80	131.80	9.80	91.13
1.571 x 10^{-5}	-520.65	722.96	180.0	128.30	8.39	92.41
2.094 x 10^{-5}	-520.28	690.36	170.30	117.90	8.01	92.75
2.618 x 10^{-5}	-520.04	526.24	162.00	90.30	6.10	94.47

The increase in the size of the semicircle as inhibitor concentration increases indicates that charge transfer is primarily involved in the control of the corrosion process (li *et al.*, 2012, Rosliza and Wan Nik, 2008). The increase in semicircular diameter that occurs with increasing DQP concentration is an indication of the formation of a thick protective film on the studied sample surface. The depressed shape of EIS curve remained unaffected with and without inhibitors showing that the mechanism remained neither interrupted nor disrupted when

different inhibitor concentrations were added to 0.5M HCl solution. Nyquist plots non-conforming to perfect semi-circle inferred the frequency dispersion owing to the substrate inhomogeneity and roughness of the metal surface (Bentiss *et al.*, 2000; Bentiss *et al.*, 2007). While the double layer capacitance (Cdl) value reduced as the concentration of DQP is increasing, the charge transfers resistance (R_{ct}) value increased as DQP concentration increased. This is in agreement with literature reports (Chakravarthy and Mohana 2014; Lebrini *et al.*, 2006). Since the local dielectric constant decreased and the electric double layer's thickness rose, it was concluded that the DQP works through adsorption at the metal-solution interface. Additionally, it is believed that the low Cdl value is caused by the progressive replacement of water molecules on the surface of the electrode with the adsorption of DQP molecules, thus lowering the extent to which metal dissolved. The Bode phase angle plots (Figure 3) show single, constant and maximum intermediate frequencies. However, the addition of an inhibitor broadens this maximum intermediate frequency. This establishes the formation of a protective coating on the metal electrode surface. The impedance electrochemical parameters calculated with ZView software on the Nyquist plot and shown in Table 3 are: solution resistance (R_1), Charge transfer resistance(R_2/ R_{ct}) and frequency maximum (f_{max}). P1 is the admittance magnitude while n1 is an exponential parameter used to calculate the amount of surface irregularity resulting from inhibitor adsorption, surface roughness, and the development of porous layers. Equation 1 determined the Double layer capacitance (Cdl) and the equation used to determine the Inhibition Efficiency (IE) (Mehdipour *et al.*, 2015:

$$Cdl = \frac{1}{2\pi \times Rct \times fmax} \quad \ldots\ldots\ldots\ldots\ldots\ldots\ldots\ldots\ldots\ldots\ 1$$

$$IE = \frac{Rct(inh) - Rct}{Rct(inh)} \times 100 \quad \ldots\ldots\ldots\ldots\ldots\ldots\ 2$$

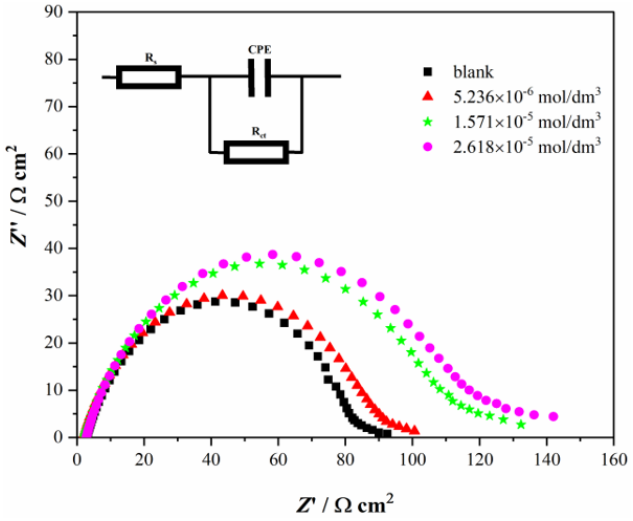

Figure 2: Nyquist plots of Mild Steel in 0.5 M HCl without and with DQP at different concentrations, temperature of 303K and immersion period of 3 hours

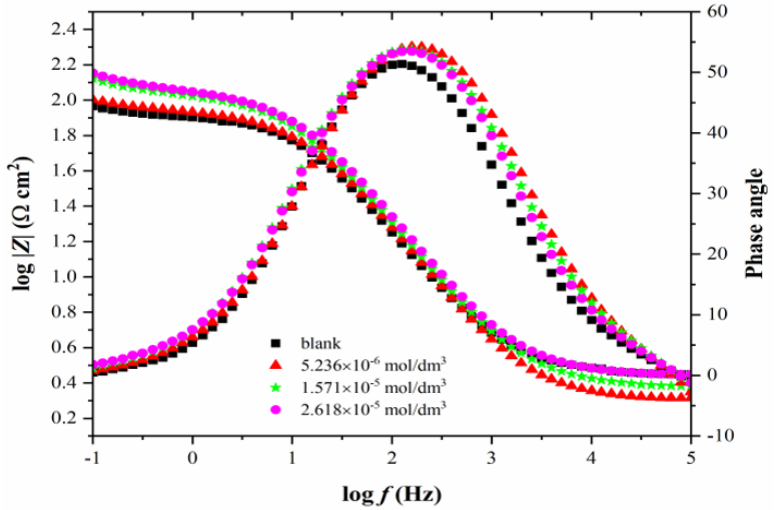

Figure 3: Bode plots of studied metal sample in 0.5 M HCl without and with DQP at different concentrations, temperature of 303K and immersion period of 3 hours

Table 3: Effect of concentrations on impedance behavior of studied metal sample in 0.5M HCl with DQP

Compound	Concentration (mol/dm3)	R1	R2	p1 (10^{-4})	n1	f (max)	IE (%)	Cdl
DQP	5.236 x 10^{-6}	2.809	82.67	3.815	0.775	12.4	97.58	1.552x10^{-4}
	1.571 x 10^{-5}	2.742	113.31	3.357	0.763	9.93	97.60	1.414x10^{-4}
	2.618 x 10^{-5}	2.370	119.63	3.644	0.759	9.93	98.02	1.339x10^{-4}

R1 =Solution resistance, R2 = charge transfer resistance, n1 = surface irregularity, p1= admittance magnitude, f max = frequency at the maximum, CPE = Constant Phase Element, (%) IE= percentage Inhibition Efficiency, Cdl is the double layer capacitance

Scanning Electron Microscope (SEM) and Energy Dispersive X-ray Spectroscopy (EDX) Analysis

The SEM analysis examines the surface morphology and ascertains the inhibitor's presence on mild steel surfaces. Figure 4 displayed the surface morphology of the studied mild steel. The EDX detector connected to the SEM evaluated the average percentages of the elements on the surface of the mild steel after seven days of immersion in 0.5 M solution of HCl without and with DQP inhibitor. Critical examination of the physical and morphological structure of images disclosed that instead of the rough, non-uniform, and corroded surface of mild steel dipped in 0.5 M HCl solution, samples containing DQP inhibitor were in a better state - they had smooth surfaces. This observation demonstrated how much slower corrosion was when DQP inhibitor was applied. The formation of a protective layer at that metal surface was observed by EDX analysis.

Figures 4 to figure 6 show the spectra of the polished mild steel surface after immersion in 0.5 M HCl solution with/without DQP and their average percentage of elements on mild steel.

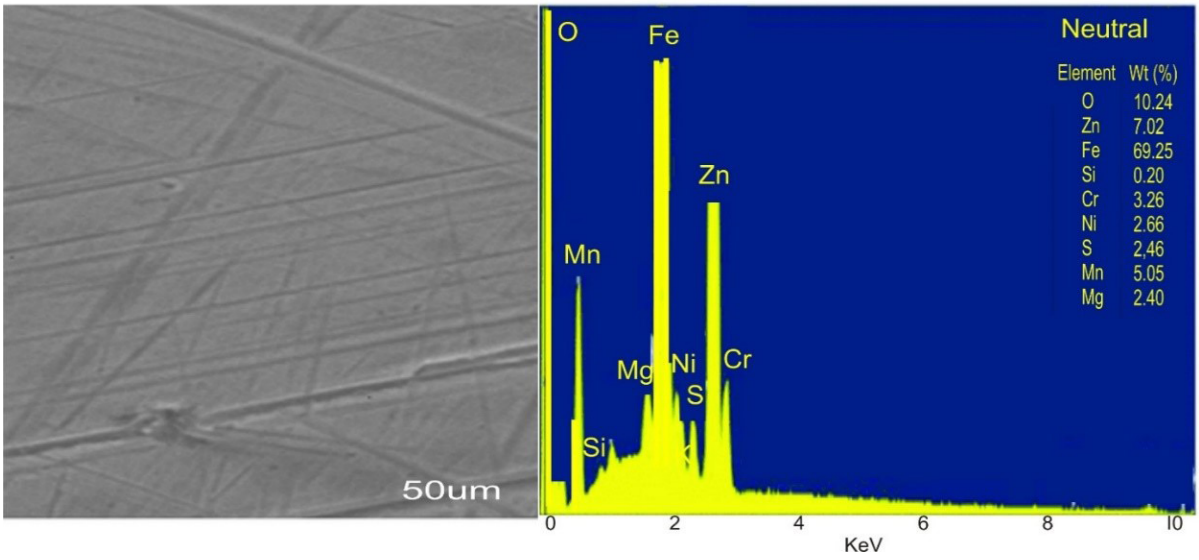

Figure 4: SEM-EDX micrograph of polished mild steel

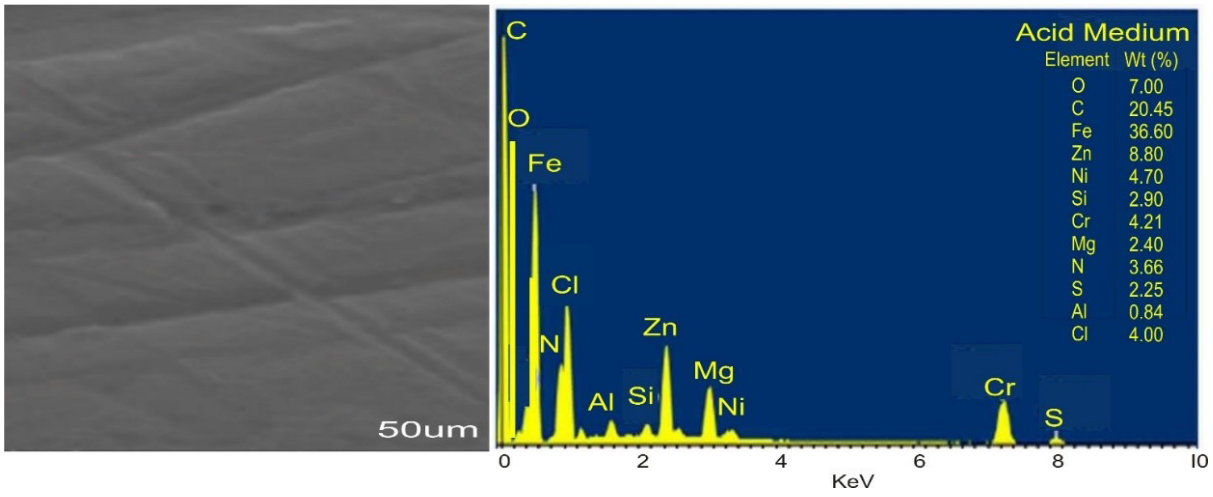

Figure 5: SEM-EDX micrograph of polished mild steel exposed to 0.5M HCl

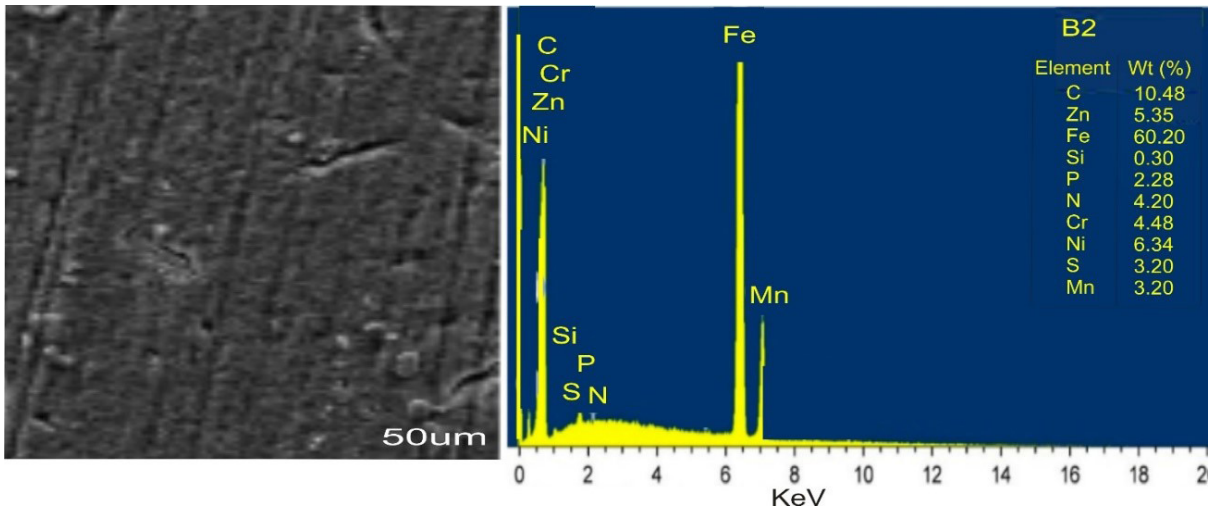

Figure 6: SEM-EDX micrograph of mild steel exposed to 5.236 x10-6 moldm-3 DQP and 0.5M HCl

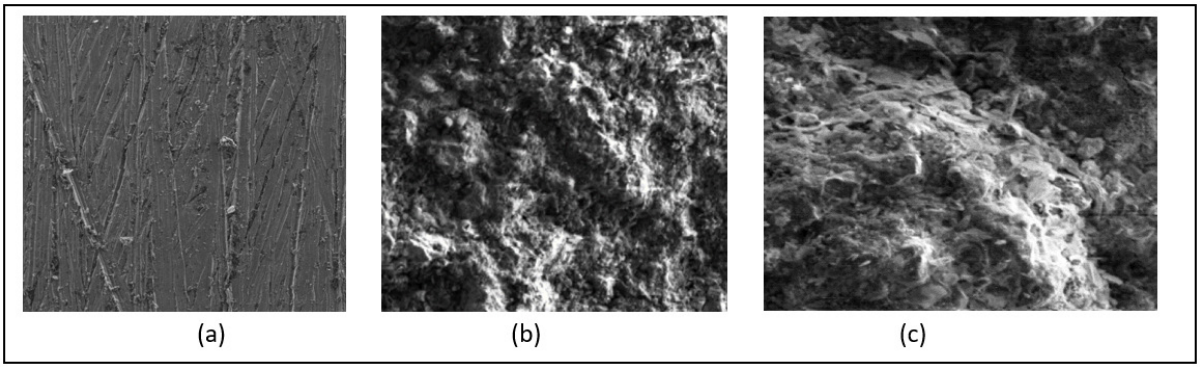

Figure 7: (a) SEM image of polished mild steel, (b) SEM image of mild steel exposed to 0.5M HCl (c) SEM image of mild steel in the presence 5.236 x 10^{-6} $moldm^{-3}$ DQP exposed to 0.5M HCl

In the present study, EDX spectra were used to estimate the percentage by weight of elements existing on the mild steel surface after seven days of immersion in the blank and solutions containing inhibitors. The elemental compositions obtained through EDX are exhibited in the right side of Figures 4,5,6

Adsorption Isotherms

Adsorption Isotherm shows the relationship between adsorbate (inhibitor/ acid solution) present in the liquid phase which is adsorbed on the surface of the mild steel acting as adsorbent (Ebenso *et al.*, 1998). It explains the basic principle and mechanism of corrosion inhibition.

The characteristics and behavior of adsorption isotherms may be obtained from this relation:

$KC = f(\theta, x) \exp(-2a\theta)$……. 3

K represents the equilibrium constant of the adsorption process, C is the inhibitor concentration in the reaction mixture (electrolyte), f(θ, x) is the configurational factor that is dependent on the physical model and the assumptions underlying the deviation of isotherms, θ is the fraction that the inhibitor can cover on the metal surface while 'x' and 'a' are the size ratio and the molecular interaction respectively.

In order to describe the behavior of the DQP inhibitor on the surface of the mild steel (adsorbate on adsorbent), the degree of surface coverage is evaluated using the weight loss of the metal involved in the corrosion process at varying concentrations of the inhibitors. Surface coverage of DQP inhibitor at different concentrations was fitted to different adsorption isotherms such as Freundlich, Langmuir, Temkin and Frumkin. The Langmuir isotherm, however, was found to be a good fit for the data acquired. Equation 4 represents Langmuir`s adsorption isotherm, which assumed that the adsorbed molecules occupy a single site and do not interact with other adsorbed species.

$C/\theta = 1/(K_{(ads)})+mC$ …….. ..…. 4

When C/θ was plotted against C (Figure 5), a straight-line graph with an intercept ($I/ K_{(ads)}$) and a slope (m) were obtained. The Adsorptive equilibrium constant ($K_{(ads)}$) was evaluated from the intercept of the plotted graph and free energy change (ΔG) was determined using equation 5 at different temperatures (Table 4)

$\Delta G = -2.303RTLog(55.5\ K\ (ads)$ ……5

The plot of C/θ against C gave fitted straight lines with slope (m) and strong linear correlations coefficient (R^2) approximately as seen in Figure 8. This shows that Langmuir's adsorption isotherm was followed during the DQP adsorption process on the surface of studied steel.

The values of free energy change (ΔG^0) using equation 5 are negative at different temperatures (Table 4), signifying that the reaction is spontaneous and feasible (Abiola and James, 2010). Researchers have earlier established that ΔG^0ads with greater negative value than 40 kJ/mol (> - 40 kJ/mol) involved electron transfer from inhibitor molecules to metal surface or charge sharing yielding a co-ordinate covalent type of chemical bond which is also referred to as chemisorption. Therefore, the adsorption isotherm for DQP, satisfied the chemical adsorption mechanism. The decrease in the adsorptive equilibrium constant (K_{ads}) value with an increase in experimental temperature indicated that DQP compound was strongly adsorbed on the surface of the mild steel coupon. The observed alternate increase and decrease in (K_{ads}) value with rising in temperature may be a result of the complex adsorptive nature of the film of the DQP compound adsorbed on the metal surface by a coordinate covalent bond with interchanging and fluctuations occurring between physical and chemical adsorption process.

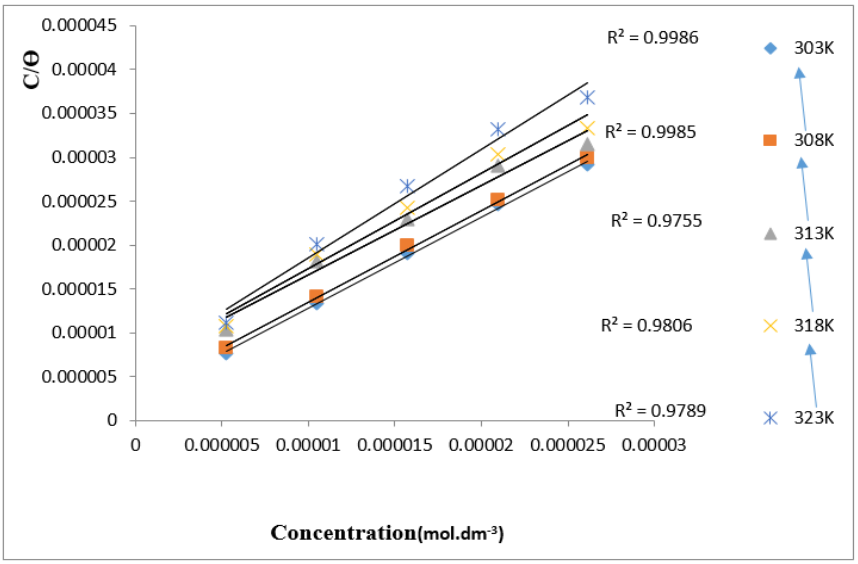

Figure 8: Langmuir adsorption Isotherm for the mild steel in 0.5M HCl without and with DQP at different temperatures

Table 4: K_{ads} and ΔG^0 (kjmol^{-1}) for DQP at different temperatures

Temperature (kelvin)	303	308	313	318	323
Adsorption equilibrium constant (K_{ads})	500,000	333,333	166,667	164,471	142,857
ΔG^0 (kjmol^{-1})	-43.183	-42.856	-41.749	-42.008	-43.082

IR Spectra of the Synthesized DQP

DQP has 86 modes of vibrations. The molecular vibrational frequencies at about 3000cm^{-1} and 3200cm^{-1} are allocated to C−H symmetric and asymmetric stretching vibrations. The frequencies at about 1690cm^{-1} and 1600cm^{-1}. C=N is responsible for the frequencies at

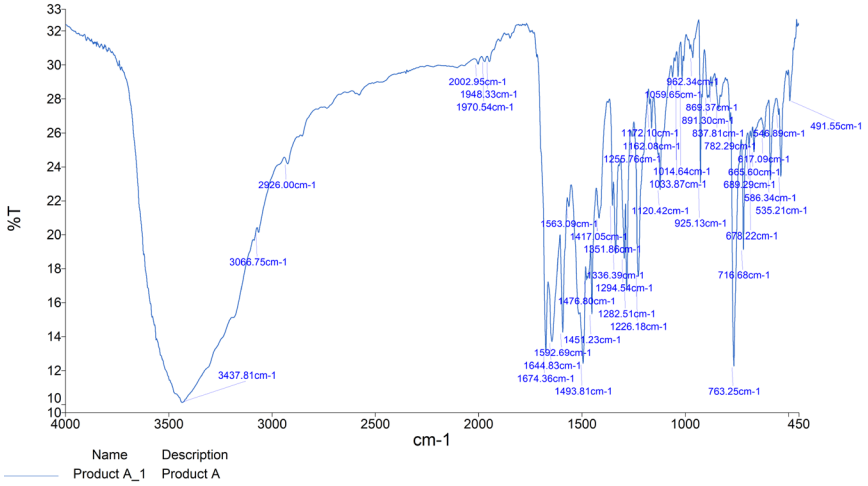

Figure 9: IR spectrum of DQP

about 1450cm^{-1} and 1600cm^{-1}. The frequencies at about 1350cm^{-1} and 650cm^{-1} are attributed to in-plane and out-of-the-plane C−H bending vibrations respectively.

The resonance effect of the phenyl ring due to the delocalization of electrons probably influenced the vibrational frequencies of the studied compounds. There is the absence of vibrational frequency peaks around 1720-1700 cm^{-1} which specifies the absence of the C=O functional group from the starting precursor carbonyl compounds.

CONCLUSION

The corrosion inhibition of mild steel in 0.5 M HCl solutions using DQP at different temperatures was examined for the first time using changes in EIS and PDP measurements. The addition of DQP at different temperatures reduced the acidic corrosion and makes DQP an effective organic inhibitor of mild steel with a maximum inhibition efficiency of 98%. Structural modification of DQP on corrosion inhibition of mild steel to advance the understanding of its inhibition mechanism and efficiency worth further investigation.

REFERENCES

Abiola, O. K. and James, A. O. (2010). The Effects of Aloe vera Extract and Kinetics of Corrosion Process of zinc in HCl Solution. *Corrosion Science, 52*, 661–664.

Adama K. K., and Onyeachu, I. B. (2022). The corrosion characteristics of SS316L stainless steel in atypical acid cleaning solution and its inhibition by1-benzylimidazole: Weight loss, electrochemical and SEM characterizations, *J. Nig. Soc. Phys. Sci., 4*, 214–222.

Bentis, F., Traisnel, M., Chaibi, N., Menari, B., Vezin, H., and Lagrenee, M. (2002). 2,5-Bis(n-methoxyphenyl)-1,3,4-oxadiazoles used as corrosion inhibitors in acidic media: correlation between inhibition efficiency and chemical structure, *Corros. Sci., 44*, 2271.

Bentiss, F, Ouanis, M, Mernari B, Traisnel M, Vezin H. Lagrenee. M, (2007). Understanding the adsorption of 4H–1,2,4-triazole derivatives on mild steelsurface in molar hydrochloric acid, *Appl. Surf. Sci., 253,* 3696–3704.

Bentiss, F; Traisnel, M and Lagrenee, M (2000). Inhibitor effects of triazoles derivatives on corrosion of mild steel in acidic media, *British Corrosion Journal, 35*(4), 315-323.

Chakravarthy M. P. and Mohana K. N. (2014). Adsorption and Corrosion Inhibition Characteristics of Some Nicotinamide Derivatives on Mild Steel in Hydrochloric Acid Solution, *ISRN Corrosion, 687276*, 13.

Chen W., Zhang J., Long G., Liu Y.and Zhang Q., (2015). From Non-Detectable to Decent: Replacement of Oxygen with Sulfur in Naphthalene Diimide Boosts Electron Transport in Organic Thin-Film Transistors (OTFT). *J. Mater. Chem. C., 3*, 8219 – 8224.

Chernick E. T., Casillas R., Zirzlmeier J., Gardner D. M., Gruber M., Kropp H., Meyer K., Wasielewski M. R., Guldi D. M. and Tykwinski R. R., (2015). Pentacene Appended to a TEMPO Stable Free Radical: The Effect of Magnetic Exchange Coupling on Photoexcited Pentacene. *J. Am. Chem. Soc., 137*, 857-863.

Ebenso, E. E., Ekpe, U. J., & Ibok, U. J. (1998). Inhibition of Mild Steel in H_2SO_4 using parica papaya Leaves Extract. *West Innovation, 10*, 52 – 59.

Gu, P. Y., Wang, Z., Xiao F. X., Lin Z., Song R., Xu Q. F, Lu J.M., Liu B., Zhang Q., (2017). an ambipolar azacene as a stable photocathode for metal-free light driven water reduction. *Mater. Chem. Front.,* 495-498.

Ismail A., Irshad H. M., Zeino A., Toor I. H., (2019). Electrochemical corrosionperformance of aromatic functionalized imidazole inhibitor under hydro-dynamic conditions on API X65 carbon steel in 1M HCl Solution. *Ara-bian Journal of Science and Engineering*, *44*, 5877.

Ito S., Hiroto S., Ousaka N., Yashima E. and Shinokubo H., (2016). Control of Conformation and Chirality of Nonplanar π-Conjugated Diporphyrins Using Substituents and Axial Ligands. *Chem. Asian J., 11*, 936-942.

Kumpawat V., Garg U., Tak R. K. (2009). Corrosion inhibition of aluminium in acid media by naturally occurring plant Artocarpus heterophyllus and Acacia Senegal. *Journal of Indian Council of Chemists, 26*, 82-84.

Lebrini M., Bentiss F., Vezin H., and Lagrenee M., (2006). The inhibition of mild steel corrosion in acidic solutions by 2, 5- bis(4-pyridyl)-1,3,4-thiadiazole: structure-activity correlation. *Corrosion Science, 48*(5), 1279–1291.

Li J., Chen S., Wang Z. and Zhang Q., (2016). Pyrene-fused Acenes and Azaacenes: Synthesis and Applications. *Chem. Rec., 16*, 1518-1530.

Li J., Zhao Y., Lu J., Li G., Zhang J., Zhao Y., Sun X. and Zhang Q., (2105). Synthesis, structure, physical properties and OLED application of pyrazine–triphenylamine fused conjugated compounds. *J. Org. Chem., 80*, 109-113.

Li Y., Jia, Z., Xiao, S., Liu, H., & Li, Y., (2016). A method for controlling the synthesis of stable twisted two-dimensional conjugated molecules. *Nat.Commun., 7*, 11637.

Li, X, Deng, S., & Fu, H., (2012). Inhibition of the corrosion of steel in HCl, H_2SO_4 solutions by bamboo leaf extract. *Corros. Sci., 62,* 163-175.

Mehdipour, M., Ramezanzadeh, B., Arman, S.Y., (2015). Electrochemical noise investigation of Aloe plant extract as green inhibitor on the corrosion of stainless steel in 1 M H_2SO_4. *J. Ind. Eng. Chem., 21,* 318–327.

Obot I. B., Solomon M. M., Onyeachu I. B., Umoren S. A., Meroufel A., Alenazi A., Sorour A. A. (2020). Development of a green corrosion inhibitor foruse in acid cleaning of MSF desalination plant. *Desalination, 495,* 114675.

Ogunyemi Babatunde Temitope and Borisade Sunday

Gbenga, (2020). Theoretical modeling of iminoisatin derivatives as corrosion inhibitors of steel in acid solution. *FUDMA Journal of Sciences, 4(*3), 672 – 678.

Patni *et al*., N. Agaruwal S. (2013) Shati Pavar: C greener approach towards Corrosion Inhibition. *Chin J. Eng.*, 1-10.

Pérez D., Peña D. and Guitián E, (2013). Aryne Cycloaddition Reactions in the Synthesis of Large Polycyclic Aromatic Compounds. *Eur. J. Org. Chem.,* 5981-6013.

Prabhu R. A., Venkatesha T. V, and Shanbhag A. V. (2008). Corrosion Inhibition effects of some Schiff's bases on mild steel in 1.0M HCl. 50(12), 3356-3382.

Rao M. R., Johnson S. and Perepichka D. F., (2016). Aromatic of Benzannulated perylene-3,9-diones: unexpected photophysical properties and reactivity, *Org. Lett., 18*, 3574-3577.

Rosliza M. and Wan Nik W.B., (2008). Improvement of corrosion resistance of AA6061 alloy by tapioca starch in seawater. *Current Applied Physics, 10*, 221-29.

Sanders S. N., Kumarasamy E., Pun A. B., Appavoo K., Steigerwald M. L., Campos L. M. and Sfeir M. Y., (2016). Exciton Correlations in Intramolecular Singlet Fission. *J. Am. Chem. Soc., 138,* 7289-7297.

Sastri V. S and Perumareddi J. R., Molecular orbital theoretical studies of some organic corrosion inhibitors. *Corrosion, 53,* 671.

Shivakumar and Mohana, (2012). Ziziphus mauritiana leaves extracts as corrosion inhibitor for mild steel in H2SO4 and HCl solutions. *European Journal of Chemistry, 3*(4), 426-432.

Ueda Y., Tsuji H., Tanaka H. and Nakamura E., (2014). Synthesis, crystal packing, and ambipolar carrier transport property of twisted dibenzo[g,p]chrysenes. *Chem. Asian J., 9*, 1623-1628.

Watanabe M., Chen K.Y., Chang Y. J. and Chow T. J., (2013). The synthesis, crystal structure and charge-transport properties of hexacene. *Acc. Chem. Res., 46,* 1606-1615.

World Steel Association, (2013). Steels contribution to a low carbon future. Retrieved from http://www.worldsteel.org/publications/position-papers/Steels-contribution-to-a-low-carbon-future.html